

Synthesis, chemical characterization and thermal behaviour of 1,2-dithiooxalato-*S,S'* complexes of Ni(II), Pd(II) and Pt(II) with 2-amino-3-methylpyridinium

Pascual Román *, Javier I. Beitia and Antonio Luque

Departamento de Química Inorgánica, Universidad del País Vasco, Apartado 644, 48080 Bilbao (Spain)

(Received 11 June 1993; accepted 28 June 1993)

Abstract

Three compounds of formula $(\text{HB})_2[\text{M}(\text{dto})_2]$, where HB^+ is 2-amino-3-methylpyridinium, dto^{2-} is 1,2-dithiooxalato-*S,S'* ligand, and M is Ni(II), Pd(II), or Pt(II), have been synthesized and characterized by elemental analysis, and infrared and UV-Vis spectroscopy. The thermal behaviour of these complexes was studied by thermogravimetry (TG) and differential thermal analysis (DTA) under argon and argon-oxygen atmospheres. The final products of the thermal decomposition were examined by elemental analysis and X-ray powder diffractometry. The IR and UV-Vis spectra indicate the presence of the aromatic cations and the complex anions. The thermal analytical data show that the starting compounds and the surrounding atmosphere significantly influence the course of the decomposition reactions, as well as the final products. In an oxidative atmosphere, a mixture of nickel(II, III) oxides and sulphides, palladium(II) oxide and metallic platinum were obtained, whereas in an inert atmosphere, nickel sulphides, palladium(II) sulphide and platinum(0) were identified as the final products.

INTRODUCTION

Interest in the coordination chemistry of square-planar d^8 metal complexes involving sulphur-donor ligands has grown in recent years because of their applications in analytical chemistry and catalysis, and their relevance to bioinorganic systems [1–4]. One of these sulphur-donor ligands is the 1,2-dithiooxalate dianion (dto^{2-} is $\text{S}_2\text{C}_2\text{O}_2^{2-}$) in which the presence of four donor atoms and the possibility of charge delocalization on its atoms results in a multifunctional ligand with unique coordination

* Corresponding author.

properties [5]. However, the studies focus mainly on the structural properties of these complexes and very little has been reported to date on their thermochemistry and thermal behaviour.

We describe herein the synthesis, chemical characterization, and thermal behaviour of three 2-amino-3-methylpyridinium salts of the square-planar inorganic metal(II) 1,2-dithiooxalato-*S,S'* anion $[M(S_2C_2O_2)_2]^{2-}$ where M is Ni(II), Pd(II), and Pt(II). In a previous paper, we have reported the crystal structure and packing of the three complexes [6]. This work is an extension of our general research programme on organoammonium salts of dithiooxalate ligand complexes [7–10] which is aimed at a more complete characterization of this kind of complex, and a deeper insight into the influence of the surrounding atmosphere and of the nature of the metal thermal decomposition processes and the final residues.

EXPERIMENTAL

Synthesis of the complexes

The dithiooxalate ligand was used as purchased from Eastman Kodak. The potassium salts of the complex anions, $[M(S_2C_2O_2)_2]^{2-}$, were prepared according to the literature method [11].

The compounds were all prepared by room-temperature mixing of aqueous solutions of 2-amino-3-methylpyridinium hydrochloride and the appropriate $K_2[M(S_2C_2O_2)_2]$ salt in an approximately 2:1 molar ratio. Immediately, an insoluble microcrystalline powder of the compound was obtained. Single crystals of the Pd compound were obtained by recrystallization in *N,N*-dimethylformamide.

Apparatus and measurements

Microanalyses of carbon, nitrogen and hydrogen were performed on a Perkin-Elmer 240 C, H and N analyser. The concentration of metal ion was determined using a Perkin-Elmer 360 atomic absorption/flame emission spectrometer. Infrared absorption spectra were recorded on an IR Beckman 4240 spectrometer using KBr discs over the wavenumber range 4000–350 cm^{-1} . UV-Vis spectra (650–220 nm) were measured in ethanol solutions (2×10^{-5} M) using a Bausch-Lomb Spectronic 2000 spectrophotometer and 1-cm silica cells. A Setaram TAG 24 S 16 thermobalance was used to obtain simultaneously the differential thermal analysis (DTA)

and thermogravimetric analysis (TG) curves in argon and argon–oxygen (4/1, v/v) atmospheres with a heating rate of $5^{\circ}\text{C min}^{-1}$. All thermal decompositions were recorded in a dynamic atmosphere with a flow rate of $50\text{ cm}^3\text{ min}^{-1}$. X-ray powder diffraction patterns of the final products were obtained on a Philips PW 1710 instrument, using graphite-monochromated Cu $K\alpha$ radiation and standard conditions, and were compared with the ASTM powder diffraction files of the Joint Committee on Powder Diffraction Standards, JCPDS [12].

RESULTS AND DISCUSSION

Table 1 gives the amounts of the synthesis reagents and the elemental analyses for the complexes isolated. The experimental data agree with the given stoichiometry of $(\text{HB})_2[\text{M}(\text{dto})_2]$ where M is the transition metal, B the 2-amino-3-methylpyridine base and dto the dithiooxalate dianion.

IR spectroscopy is a good technique for confirming the presence of the protonated organic cations and the complex anions. The three IR spectra are quite similar with respect to the bands corresponding to the 2-amino-3-methylpyridinium cations. The absorption bands at around 3000 and 2700 cm^{-1} are attributable to the C–H and N–H groups, respectively. The other characteristic bands of this cation were obtained between 1650 and 600 cm^{-1} . As expected from literature data [5, 7–10, 13], the bands corresponding to the anions of the complexes are detectable in the 1600 – 350 cm^{-1} range and the slightly discrepancies between the three compounds are due to the different metal ions. Table 2 shows the infrared bands for the complex anions with the corresponding assignments.

UV–Vis spectra of the three compounds (Table 3) show absorptions at around 295 and 230 nm , attributable to the $\pi \rightarrow \pi^*$ and $n \rightarrow \pi^*$ transitions of the 2-amino-3-methylpyridinium cations [14] which are not affected by the complex anions. The remaining spectral bands correspond to electronic transitions in the complex anions [15, 16] and the discrepancies are owing to the existence of different M–S bonds. For the $[\text{Pd}(\text{S}_2\text{C}_2\text{O}_2)_2]^{2-}$ complex, the $M \rightarrow L(\pi^*)$ and $d_{xy} \rightarrow d_{x^2-y^2}$ bands are probably masked by the very intense $L \rightarrow M$ band at 278.5 nm [15].

The TG, DTG and DTA curves of the three compounds under argon–oxygen and argon atmospheres are shown in Figs. 1–3. The data given in Table 4 were obtained from these curves.

The thermoanalytical results show that the thermal processes and the final residues are strongly influenced by the nature of the atmosphere and the starting compound. No stable intermediate products could be found during the thermal decomposition owing to its complexity and to the overlap of the processes in both atmospheres.

In the oxidative atmosphere, the Ni(II) complex undergoes decomposition in an exothermic process between 215 and 285°C , attributable to the

TABLE 1
 Synthesis reagents and elemental analyses of the complexes

Complex	Colour	Reagent/g (mmol)		Yield/%	Analysis, calc. (found)/%			
		BCl	$K_2[M(dto)_2]$		C	H	N	M
$(HB)_2[Ni(dto)_2]$	Dark purple	0.40 (2.77)	0.50 (1.33)	86	37.15 (37.17)	3.51 (3.54)	10.83 (10.81)	11.35 (11.32)
$(HB)_2[Pd(dto)_2]$	Yellow	0.40 (2.77)	0.48 (1.13)	85	34.01 (34.02)	3.21 (3.24)	9.92 (9.90)	18.84 (18.80)
$(HB)_2[Pr(dto)_2]$	Yellow-red	0.06 (0.41)	0.10 (0.19)	89	29.40 (29.44)	2.78 (2.81)	8.57 (8.53)	29.84 (29.83)

TABLE 2

IR bands (cm^{-1}) for the $[\text{M}(\text{dto})_2]^{2-}$ anions

Ni(II)	Pd(II)	Pt(II)	Assignment
1560(vs)	1580(vs)	1580(vs)	$\nu(\text{C}=\text{O})$
1430(s)	1435(s)	1440(s)	$\nu(\text{C}=\text{O})$
1095(vs)	1095(vs)	1090(s)	$\nu(\text{C}=\text{C}) + \nu(\text{C}-\text{S})$
950(s)	945(s)	940(s)	$\delta(\text{C}=\text{O}) + \nu_{\text{as}}(\text{C}-\text{S})$
600(m)	600(m)	575(w)	$\nu(\text{C}-\text{S})$
440(w)	420(m)	440(w)	$\nu(\text{C}-\text{S})$
420(w)	410(w)	420(w)	$\nu_{\text{as}}(\text{M}-\text{S})$
370(w)	370(w)	350(w)	$\nu_{\text{s}}(\text{M}-\text{S})$

Key: vs, very strong; s, strong; m, medium; w, weak; ν , stretching tension; δ , deformation mode; s, symmetric; as, asymmetric.

TABLE 3

UV-Vis spectra of the complexes, EtOH, λ/nm ($\epsilon \times 10^{-3}/\text{M}^{-1} \text{cm}^{-1}$)

$(\text{HB})_2[\text{Ni}(\text{dto})_2]$	$(\text{HB})_2[\text{Pd}(\text{dto})_2]$	$(\text{HB})_2[\text{Pt}(\text{dto})_2]$	Assignment
571.1 (2.4)		468.7 (4.5)	$\text{M} \rightarrow \text{L}(\pi^*)$
571.1 (2.4)		339.4 (3.0)	$d_{xy} \rightarrow d_{x^2-y^2}$
510.3 (5.1)		435.7 (5.6)	$\text{M} \rightarrow \text{L}(\pi^*)$
		417.7 (5.1)	
296.1 (40.3)	388.7 (8.2)		$\text{L}(\pi) \rightarrow \text{M}$
254.8 (27.3)	233.9 (25.8)	233.7 (26.5)	$\text{L}(\pi) \rightarrow \text{L}(\pi^*)$
228.7 (27.3)	278.5 (38.4)		$\text{L}(\sigma) \rightarrow \text{M}$
296.1 (40.3)	290.9 (6.3)	293.9 (9.3)	$\pi \rightarrow \pi^*$
228.7 (27.3)	233.9 (25.8)	233.7 (26.5)	$n \rightarrow \pi^*$

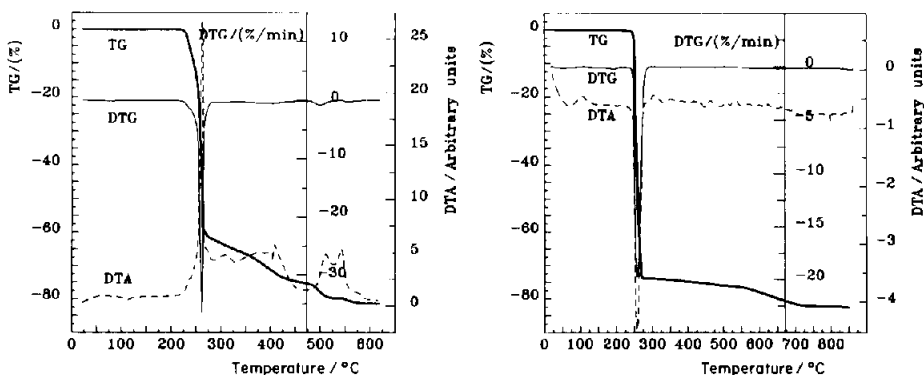


Fig. 1. RG-DTG-DTA curves for the thermal decomposition of $(\text{HB})_2[\text{Ni}(\text{dto})_2]$ in argon-oxygen (left) and argon (right) atmospheres.

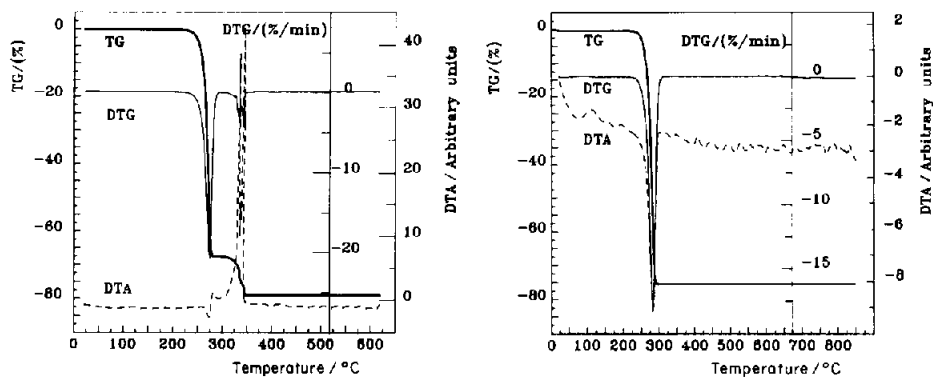


Fig. 2. Thermal decomposition of $(\text{HB})_2[\text{Pd}(\text{dto})_2]$ in argon–oxygen (left) and argon (right) atmospheres.

pyrolysis of the organic cations and the breakdown of the dithiooxalato ligands. The decomposition continues with a progressive weight loss, without clear peaks in the DTA and DTG curves, and two exothermic processes corresponding to reactions of the inorganic residues. The X-ray powder diffraction pattern of the final stable solid residue, obtained above 600°C , mainly corresponds to the Ni(II) sulphide (JCPDS file 2-1280), but also shows the presence of some diffraction maxima which could be attributed to different nickel oxides and sulphides (NiO , Ni_2O_3 and Ni_2S_3). In argon atmosphere, the complex is stable up to 225°C where an abrupt weight loss takes place corresponding to a strong endothermic peak in the DTA curve. This process is followed by a progressive weight loss up to 735°C , after which there is no further weight loss on the TG curve. An X-ray diffraction study of the final black residue, whose elemental analysis did not reveal the presence of carbon, exhibited peaks due to stoichiometric NiS, in addition to other peaks not recorded in the JCPDS files, which may

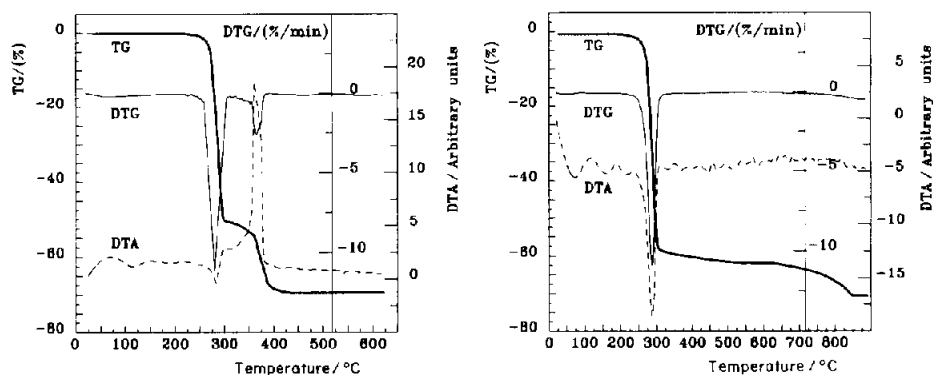


Fig. 3. TG–DTG–DTA curves for the thermal decomposition of $(\text{HB})_2[\text{Pt}(\text{dto})_2]$ in argon–oxygen (left) and argon (right) atmospheres.

TABLE 4

Thermal analysis data for the compounds in argon–oxygen and argon atmospheres

Ar + O ₂					Ar				
Step	T _i /°C	T _f /°C	T _m /°C ^a	Δm/% ^b	Step	T _i /°C	T _f /°C	T _m /°C ^a	Δm/% ^b
(HB)₂[Ni(dto)₂]									
1	215	285	265(+)	62.42	1	225	280	260(-)	74.65
2 ^c	285	480		12.35	2 ^c	280	735		7.75
3	480	525	510(+)	4.30					(82.40)
4	525	570	545(+)	1.65					
5 ^c	570	600		0.62					
				(81.34)					
(HB)₂[Pd(dto)₂]									
1	235	285	275(-)	66.86	1	230	300	280(-)	75.03
2 ^c	285	320		0.70					(75.03)
3	320	335	330(+)	5.59					
4	335	345	340(+)	5.27					
				(78.42)					
(HB)₂[Pt(dto)₂]									
1	230	295	280(-)	50.25	1	200	315	290(-)	57.80
2 ^c	295	350		4.24	2 ^c	315	860		12.27
3	350	425	370(+)	15.03					(70.07)
				(69.52)					

^a Endothermic (-) or exothermic (+) process. ^b Total mass losses are shown in parentheses.^c Progressive mass loss without clear peaks in DTG and/or DTA curves.

be ascribed to non-stoichiometric sulphides; this behaviour is well known for metallic sulphides heated in an inert atmosphere [17].

The thermal decomposition of the Pd(II) compound under argon–oxygen atmosphere starts above 235°C with an endothermic stage which is followed by a progressive weight loss and two strong exothermic peaks in the DTA curve up to 350°C. The final stable residue was identified as palladium(II) oxide (ASTM 6-0515). No palladium or palladium sulphide could be detected. In the inert atmosphere, the thermal degradation occurs in an endothermic step between 230 and 300°C. The chemical analysis of the final residue gives no indication of carbon, nitrogen or hydrogen in its composition, and it was identified as palladium(II) sulphide (ASTM 10-429).

The TG curve of the Pt(II) complex in the oxidative atmosphere shows that the compound is stable up to 230°C, when a first weight loss takes place corresponding to an endothermic peak centred at 280°C on the DTA curve. The decomposition ends with a strong exothermic process below 425°C which leads to platinum(0) (ASTM 4-802) as final product. Platinum is also the final product of the thermal degradation in inert atmosphere, but is obtained above 860°C.

CONCLUSIONS

The thermal decompositions of the metallic complexes described in this paper are not simple and the processes generally involve overlapping steps which, together with the great diversity of possible intermediate products, precludes exhaustive interpretations. Only the final products could be identified by elemental analysis and X-ray powder diffraction. These residues depend on the atmosphere for the Ni(II) and Pd(II) complexes. For the first, a complex mixture of nickel(II, III) oxide and sulphide is obtained under oxidative atmosphere, but nickel(II) sulphide and non-stoichiometric nickel sulphide are formed in inert atmosphere. PdO and PdS are obtained from the Pd(II) complex in oxidative and inert atmospheres, respectively. In the case of the Pt(II) complex, the course of the thermal degradation is different in both atmospheres, but the final residue is metallic platinum.

ACKNOWLEDGEMENT

This work was financially supported by the UPV/EHU (Grant No. 160.310-EA166/92) project.

REFERENCES

- 1 W. Dietzsch, P. Strauch and E. Hoyer, *Coord. Chem. Rev.*, 121 (1992) 43.
- 2 A. Müller, *Polyhedron*, 5 (1986) 323.
- 3 G. Wilkinson, R.D. Gillard and J.A. McCleverty (Eds.), *Comprehensive Coordination Chemistry*, Vol. 6, Pergamon Press, New York, 1987, pp. 541–1027.
- 4 R.H. Holm, *Acc. Chem. Res.*, 10 (1977) 427.
- 5 D. Coucouvanis, N.C. Baezinger and S.M. Johnson, *J. Am. Chem. Soc.*, 95 (1973) 3875.
- 6 P. Román, J.I. Beitia and A. Luque, *Acta Crystallogr.*, 49 (1993) 584.
- 7 P. Román, A. Luque, J.I. Beitia and C. Guzmán-Mirallas, *Polyhedron*, 11 (1992) 1883.
- 8 P. Román, J.I. Beitia, A. Luque and J.M. Gutiérrez-Zorrilla, *Mater. Res. Bull.*, 27 (1992) 339.
- 9 P. Román, J.I. Beitia, A. Luque and A. Aranzabe, *Polyhedron*, 12 (1993) 1345.
- 10 P. Román, J.I. Beitia and A. Luque, *Polyhedron*, in press.
- 11 E.G. Cox, W. Wardlaw and K.C. Webster, *J. Chem. Soc.*, (1935) 1475.
- 12 Powder Diffraction File (1982), Powder Diffraction File of the Joint Committee on Powder Diffraction Standards, Sets 1-32, published by the International Center of Diffraction Data, Swarthmore, PA 19081.
- 13 J. Fijita and K. Nakamoto, *Bull. Chem. Soc. Jpn.*, 37 (1964) 528.
- 14 R.C. Weast and M.J. Astle (Eds.), *CRC Handbook of Chemistry and Physics*, 59th edn., CRC Press, Boca Raton, FL, 1978.
- 15 A.R. Latham, V.C. Hascall and H.B. Gray, *Inorg. Chem.*, 6 (1965) 788.
- 16 R. Czernuszewick, D.P. Strommen and K. Nakamoto, *Inorg. Chim. Acta*, 34 (1979) L21.
- 17 J.J. Criado, B. Macías and M. Castillo, *Thermochim. Acta*, 127 (1988) 101.